



Fully automated focused infrared microashing combined with use of ICP-based instruments for rapid analysis of multiple elements in biological samples

Ni Zhang^{1,2} · Jianbin Zheng¹

Received: 22 October 2017 / Revised: 21 November 2017 / Accepted: 27 November 2017 / Published online: 22 December 2017
© Springer-Verlag GmbH Germany, part of Springer Nature 2017

Abstract

A fully automated focused infrared microashing sample preparation system was proposed for preparation of biological samples with high organic matter content for the determination of multiple elements combined with inductively coupled plasma optical emission spectroscopy and inductively coupled plasma mass spectrometry. The whole ashing procedure, including sample transfer, carbonization and oxidation of the sample, dissolution of ash, constant volume control, and homogenization of the solution, was automatically controlled. Gold-plated infrared tubes were used to produce and focus infrared radiation to heat the sample. Ozone was used to accelerate the carbonization of samples at a lower temperature to avoid the production of large amounts of empyreumatic oil. In addition, the self-designed double-layer tube serves as a site for ashing and carbonization of the sample and as a container for dissolving ash, as well as for holding the solution. This is the only container in the entire system to reduce the risk of pollution. Eight biological certified reference materials were used as examples to evaluate the performance of the proposed device. A sample ashing pretreatment cycle, from solid sample to liquid solution, took only 40 min and simultaneously treated 12 samples. Except for individual results, the relative errors between the certified values and recorded values for 38 micro and trace elements, including Ca, Mg, Na, P, Li, Be, Sc, Ti, V, Mn, Co, Ni, Cu, Zn, Rb, Sr, Y, Mo, Ag, Cs, Ba, Tl, Th, U, and rare earth elements, were typically less than 30%. The relative standard deviations for five determinations were typically less than 15%.

Keywords Automated ashing · Infrared heating · Sample preparation · Inductively coupled plasma · Biological samples

Introduction

There has been rapid development of high-performance elemental analysis instruments, such as inductively coupled plasma (ICP) optical emission spectroscopy (OES) and ICP mass spectrometry (MS) instruments. Instrument detection limits have been greatly reduced and detection speed has been greatly increased. Because sample preparation takes up most of

the time, it has become a bottleneck for the entire analysis process [1].

Wet digestion and dry ashing are two classical and conventional sample preparation methods for ICP-based analysis [2–6]. Compared with wet digestion, dry ashing has many advantages for preparation of samples with high organic matter content. First, the acidity of the final solution can be easily controlled to meet the requirements of ICP-based instruments, especially ICP-MS instruments [7]. Second, organic matter samples, which interfere with ICP-OES and ICP-MS measurement, including polyatomic interferences, an enhancement effect on some hard-to-ionize elements, and carbon deposits [8–10], can be removed easily [11]. Third, it is environmentally benign because large amounts of strong acids are not used [12].

In recent decades, different methods of dry ashing have been developed. These methods use different ways of heating: electricity, microwaves, plasma, ultraviolet light,

Electronic supplementary material The online version of this article (<https://doi.org/10.1007/s00216-017-0790-z>) contains supplementary material, which is available to authorized users.

✉ Jianbin Zheng
zhengjb@nwu.edu.cn

¹ Institute of Analytical Science, Shaanxi Provincial Key Laboratory of Electroanalytical Chemistry, Northwest University, Xi'an, Shaanxi 710069, China

² Xi'an Northwest Geological Institute for Nonferrous Metals Co. Ltd., 25 Xiying Road, Xi'an, Shaanxi 710054, China

and laser [7]. However, these dry ashing methods have disadvantages, which were described in our previous review: they are time-consuming, they are energy-consuming, they have a high cost, they have a low throughput, or the device is large [13].

In our previous report, a focused infrared ashing system was proposed for sample ashing for the first time. Gold-plated infrared quartz tubes were used as heating elements to produce and focus infrared radiation onto the sample zone. The flow-through ashing tube was used to ensure oxygen penetrated throughout the entire sample layer, thus increasing the efficiency of sample oxidation [14]. A single ashing step is generally completed within 30 min. Although the novel ashing system has the advantages of small size, fast heating rate, and a durable heating element, some of the disadvantages of dry ashing methods are still not resolved. In the system, the ashing of sample and the dissolution of ash uses two different containers. In addition, the flow-through ashing tube used has an open structure, making the whole ashing process susceptible to exogenous contamination. The whole ashing process, including sample transfer, carbonization and oxidation of the sample, dissolution of ash, constant volume control, and homogenization of the solution, cannot be automated. Errors resulting from manual operation are still not eliminated.

In this study, a fully automated focused infrared microashing sample preparation system (AFIA) was firstly constructed and developed for the simultaneous determination of multiple elements combined with ICP-OES and ICP-MS. The whole ashing process simultaneously treated 12 samples and was automatically completed by unattended operation within 40 min, combined with focused infrared radiation heating, ultrasonic dissolution of the ash, and ultrasonic homogenization and bubble agitation of the solution. A double-layer quartz tube was designed and used in the whole ashing process as the only vessel, serving as the site for carbonization and oxidation of the sample, and as a container for dissolving ash. The single vessel is less likely to be affected by exogenous contamination than multiple vessels. Moreover, the double-layer tube also significantly reduced the risk of contamination from the ashing process. Also, at the carbonization stage, ozone was used as an auxiliary gas to achieve carbonization of the sample at lower temperatures in a relatively short time [15], and to inhibit the generation of empyreumatic oil.

The AFIA operating conditions, including heating temperature, heating time, gas flow rates, and ultrasonic time, were optimized. Eight different biological certified reference materials were used to evaluate the accuracy of the proposed method. The samples were ashed by the AFIA, and ICP-OES or ICP-MS was used to determine the contents of elements in the resulting solution.

Materials and methods

Instrumentation

The details of the AFIA are shown in Fig. 1. The system (140 cm long, 75 cm wide, and 120 cm high) is composed mainly of an infrared heating furnace, an ashing tube assembly, an ultrasound module, a multichannel gas module, a solution injection module, and a manipulator.

The infrared heating furnace (Fig. 2) includes a heating chamber and three infrared quartz tubes (single tube size, 380 mm long, 30 mm wide, and 8 mm high). The heating chamber was made of mullite refractory and has 12 orifices (30-mm diameter) on its upper surface for insertion of the ashing tubes. There were two inlets for the cooling gas at the front end of the chamber. Three infrared quartz tubes provide uniform heating with 12 orifices for ashing tubes. One was transparent, and the others were semi-gold-plated. The tolerable temperature of the gold plating layer is 980 °C. The heating concentrated zone was a region with a width of 30 mm. The temperature was achieved by means of an armored K-type thermocouple. The ashing tube assembly consisted of 12 quartz ashing tubes and a tube shelf (Fig. 2). The ashing tube was designed as a double-layer structure including an inner tube and an outer tube. The inner tube depicted in Fig. 2 had two open ends, a polytetrafluoroethylene interface (a cylindrical sleeve) and a P40-grade quartz sand core with 16–40- μm bore diameter as a sample holder [16]. The outer tube was open only at the upper end and also had a polytetrafluoroethylene interface. The upper ends of the inner tube and the outer tube extended outward. The inner and outer tubes crossed through the polytetrafluoroethylene interface and then were blocked at the upper ends of the tube, respectively. The inner tube could be inserted into the outer tube.

The tube shelf is a three-layer structure. The interfaces closely connected the inner and outer tubes to the tube shelf, keeping the tubes stable. The inner tube is fixed in the first layer, and the outer tube is fixed between the second and third layers. The first layer of the tube shelf could be separated from the second and third layers by a manipulator. The tube shelf was able to accommodate 12 ashing tubes at a time. The polytetrafluoroethylene interfaces and ashing tubes are all reusable. The sample was weighed and placed on the sample holder. When the ashing tube was vertically inserted into the heating chamber, the holder was in the position of the heating zone (Fig. 2).

The multichannel gas module has 12 gas channels to provide gas with the same flow rate to every ashing tube. The gas module and inner tube were sealed by a silicone pad. An ozonator (ZA-D, Zeao, Guangzhou, China) was used to supply ozone with a concentration of 0.05 g L⁻¹ continuously. An ultrasonic cleaner (KM-36B, Kejiemeng, Guangzhou, China), which has a power of 180 W and a ultrasonic frequency of 40

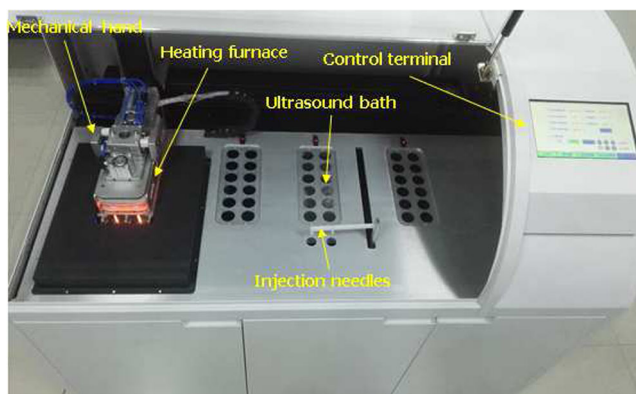


Fig. 1 Photograph of the fully automated focused infrared microashing sample preparation system

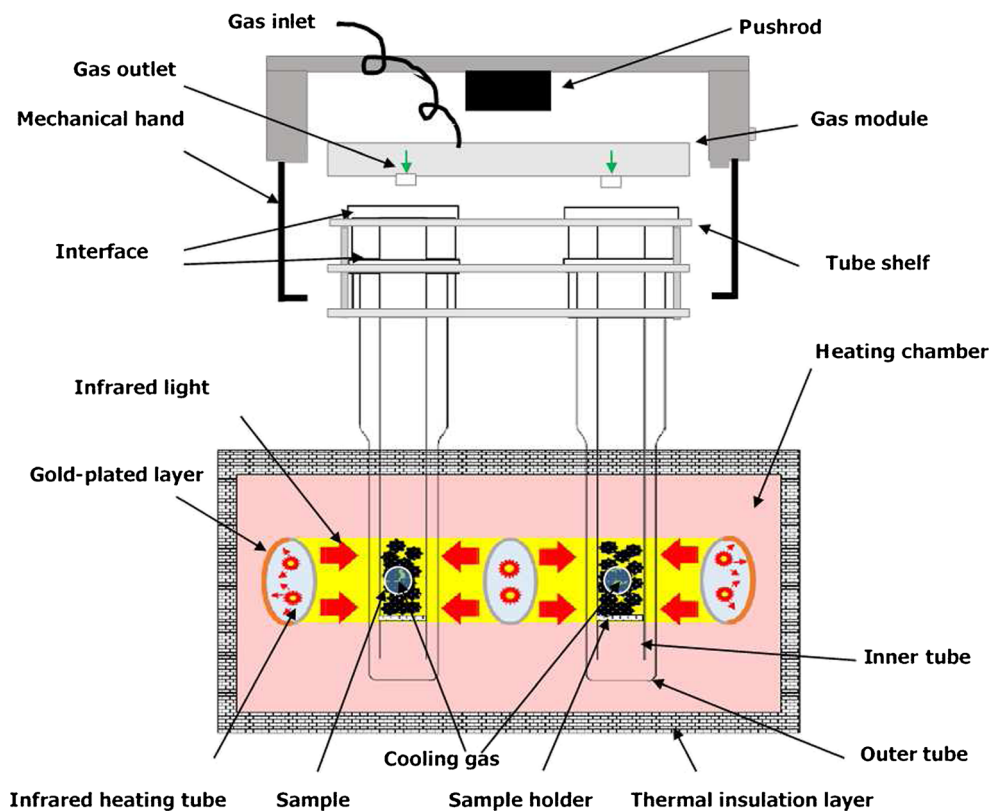
kHz, was used to assist in dissolving ashes and homogenizing solutions with water as the ultrasonic propagation medium. Two syringe pumps (SMD02-1, Longer, Baoding, China) were used to provide a quantitative solution. The manipulator consisted of an open-close cylinder and a push-down cylinder (Fig. 2). The open-close cylinder could complete the grabbing of the module, and the push-down cylinder could exert pressure on the silicone pad of the gas module, thereby ensuring the sealing of the gas module and the inner tube. The whole manipulator could be moved up, down, left, and right through a longitudinal and a transverse slide rail.

All modules communicated via a controller area network bus. The system automatically executed the whole sample

preparation program via a host computer, including sample transfer, heating of the sample, dissolution of the ash, constant volume control, and homogenization of the solution.

The determination of multiple elements was performed with an ICP optical emission spectrometer (iCAP MFC 6300 Radial, Thermo Fisher Scientific, Waltham, MA, USA) and a 7700x ICP mass spectrometer (Agilent Technologies, Santa Clara, CA, USA). The ICP-OES instrument has a high-resolution echelle optical system and a charge injection device array detector, with an extended spectral range of 166–847 nm and axial plasma view. Appropriate solutions were introduced into the plasma by a conventional sample introduction system that includes a quartz concentric nebulizer, a cyclonic spray chamber, and a quartz torch. The ICP-MS instrument, equipped with a quartz concentric nebulizer and a Scott-type double pass spray chamber, was used for detection of trace and ultratrace elements. The spray chamber temperature was precisely maintained with a thermoelectric (Peltier) device. An octopole collision/reaction system was used to reduce polyatomic ion interferences with helium as the collision gas [17]. Instrument drift or sample-matrix-induced interferences were corrected for by the application of the internal standards of ^{103}Rh for ^7Li to ^{137}Ba , and ^{185}Re for ^{139}La to ^{238}U . The internal standards were mixed online with the sample solution before nebulization with use of a three-channel mixing coil. All glassware was soaked in 10% (v/v) nitric acid for 24 h and washed with deionized water and dried in an air oven before

Fig. 2 The heating furnace and the ashing tube assembly



use. The instrument and the air oven are kept in a class 1000 cleanroom. All sample handling before analysis was performed under class 100 conditions.

Reagents

Nitric acid (69%, ultrapure reagent, total metals less than 10 ng mL⁻¹) was purchased from Suzhou Jingrui Chemical Co. (Suzhou, China). Compressed oxygen gas of 99.5% purity and argon gas of 99.999% purity (Shaanxi Xinding Co., Xi'an China) were used as working gases. Water with a resistivity of 18.2 MΩ cm was obtained from a Millipore water purification system. (Millipore Filter Co., Bedford, MA, USA)

The multielement standard stock solutions for ICP-MS were purchased from SPEX CertiPrep (Metuchen, NJ, USA). Calibration standards were freshly prepared by appropriate dilution of the stock solution (10 mg L⁻¹). The standard stock solutions for ICP-OES were purchased from Central Iron & Steel Research Institute (Beijing, China). The calibration standards were prepared by diluting the stock solutions of Ca, Mg, and Na (all 500 mg L⁻¹) and P (1000 mg L⁻¹)

The certified reference materials (GBW10020 citrus leaf, GBW07603 bush leaf, GBW10049 scallion, GBW10028 astragalus, GBW10023 laver, GBW10012 maize, GBW09101b human hair, and GBW10024 scallop) were purchased from the Chemical Metrology & Analytical Science Division, National Institute of Metrology, China.

Analysis procedure

All powder samples were dried at 60 °C for 4 h in a forced air oven before use. Twelve quartz ashing tubes were placed and were fixed in the tube shelf by polytetrafluoroethylene interfaces. A sample mass of 200 mg was accurately weighed in the 12 quartz inner tubes. The tube shelf and the gas module were placed in the respective initial positions (Fig. 1). The AFIA was run automatically according to a preset program described in Table 1. The gas module was moved on the top of the sample shelf, and the sealing of the gas module and the inner tube was ensured by pressure on the silicone pad with a pushrod. After the optimized heating program had been completed, the cooling gas was injected into the chamber. Then, the gas module was moved to its initial position, and the whole tube shelf was placed into the ultrasonic bath. Next, the syringe pumps automatically injected 25 mL of 10% (v/v) nitric acid into each sample tube. Afterward, the ultrasound module started to work, and the gas module was moved on the tube shelf. After the ash had dissolved completely, oxygen was injected into the inner tube. By adjustment of the appropriate oxygen pressure, the solution in the inner tube and a small amount of oxygen were pressed out of the outer tube. The elements in the solution were homogenized by synergistic action of ultrasonic and gas agitation. Then, the pushrod of

the push-down cylinder was retracted and the oxygen inlet was closed. The seal of the inner tube was lost. At this point, the pressure in the inner tube gradually reduced to atmospheric pressure, and the solution in the outer tube flowed back to the inner tube. At this point, a cycle of the homogenization process was completed. After these actions had been repeated three times, a homogeneous solution was obtained (a video of the AFIA running is provided in the [electronic supplementary material](#)). All the resulting solutions were analyzed directly by ICP-OES and ICP-MS.

Results and discussion

The effect of the double-layer ashing tube

The ashing tube was designed as a double-layer structure consisting of an inner tube and an outer tube, mainly considering three aspects:

1. During the whole ashing process, a single vessel facilitates the automation of the ashing process. Further, it reduces mechanical movement of the vessel, and shortens the run time. The single vessel must have two functions: (1) to be used as a site for ashing and carbonization of the sample and (2) to serve as a container for dissolving ash and for the solutions. In our previous report, the flow-through ashing tube was used to ensure oxygen penetrated the entire sample layer, thus increasing the efficiency of sample oxidation [18]. Because both ends of the flow-through ashing tube were open, it could not contain solutions and dissolving ash. Therefore, an outer tube with an opening at only one end was used (Fig. 2).
2. In the conventional ashing process, carbonization and oxidation of samples is performed in a crucible. After the ash has dissolved, the resulting solution is transferred to another container (i.e., a volumetric flask or a colorimetric tube) for analysis. The whole ashing process requires the use of multiple vessels. As a result, the risk of sample contamination by multiple vessels is increased. In addition, the analyte is subjected to multiple transfer operations throughout the ashing pretreatment process, thereby increasing the probability that the analyte was exposed to the working environment. Eventually, the risk of contamination of the sample by the external environment increases. However, a double-layer ashing tube was used in this work. It consisted of an inner tube and an outer tube. The inner tube acted as an ashing crucible, while the outer tube was a container for the solution. The double-layer ashing tube was the only vessel in the whole ashing process, avoiding the risk of increasing pollution by the use of many vessels. Moreover, compared with conventional open heating in a heating chamber, the semisealed

Table 1 The optimized operating parameters of the automated focused infrared microashing sample preparation system

Step	Function	Temperature (°C)	Time (min)	Gas/flow rate (mL min ⁻¹)
1	Carbonization	20–250	10	O ₃ /50
2	Oxidation	600	20	O ₂ /600
3	Removal of empyreumatic oil	600	5	O ₂ /100
4	Injection of solution	25	2	–
5	Ultrasound homogenization and blowing of gas	25	3	O ₂ /250

structure of the double-layer ashing tube also significantly reduced exogenous pollution from the interior atmosphere of the heating chamber and cross-contamination between samples. Compared with the conventional muffle ashing method, the proposed method greatly reduces sample contamination. In the sample blank acquired after the pretreatment by the proposed method, the concentrations of elements such as Ni, Co, Zn, and Na, which are easily contaminated by traditional ashing methods, are almost equal to those in the reagent blank. For micro and trace elements, the blank concentrations of most elements were less than 0.01 ng mL⁻¹, except for the blank concentrations of Sr, Ba, V, and Zn, which were 0.1, 0.2, 0.2, and 0.03 ng mL⁻¹, respectively.

- For the double-layer ashing tube, the auxiliary gas was injected from the upper end of the inner tube and passed through the sample holder, and then flowed into the outer tube from the lower end of the inner tube. Finally, it flowed out from the upper end of the outer tube. The empyreumatic oil produced during the carbonization and oxidization process would flow from the inner tube to the outer tube with the auxiliary gas. The empyreumatic oil would pass through the heating zone twice, thus increasing the probability of empyreumatic oil being pyrolyzed. Therefore, the double-layer ashing tube was favorable for the removal of empyreumatic oil.

The inner tube was of the flow-through design in our previous report [13]. It was open at both ends. A quartz sand core with a bore diameter of 16–40 μm was sintered on the inner wall of the inner tube as a sample holder. To realize the function of dissolving ash and containing the solution of the ashes, the outer tube was designed to have only an upper opening. The inner tube was inserted in the outer tube (Fig. 2). In the process of dissolving and homogenizing the ash, the solution was pressed into the outer tube by the blowing of gas into the inner tube, and was homogenized by ultrasound. When the ashing tube was inserted into the heating furnace, the sample holder was located at the center of the heating zone. At the

same time, when the 25-mL solution was completely pressed from the inner tube into the outer tube, it did not overflow the outer tube.

Conditions for carbonization with the aid of ozone

In general, conventional ashing methods require a carbonization process in an anoxic or anaerobic environment that involves the use of an electric heating plate before oxidation in a muffle oven [19]. After the graphitization process, the sample becomes a carbon-rich material [20]. The main purpose of carbonization is to (1) prevent the sample from burning at high temperatures, resulting in the sample splashing; (2) prevent easy-foaming materials (such as sugar, protein, starch) from expanding at high temperatures and overflowing the vessel; and (3) prevent the carbon particles from being easily wrapped, making the ashing incomplete.

In general, the carbonization time decreases as the carbonization temperature increases, while empyreumatic oil production increases as the carbonization temperature increases. During the dissolution of ash, the empyreumatic oil produced is partially dissolved in the solution. The organic matter in the empyreumatic oil can interfere with ICP-based instrument measurements, including polyatomic interferences, an enhancement effect on some hard-to-ionize elements, and carbon deposits, and is not conducive to the cleaning of ashing tubes. Therefore, the carbonization temperature cannot be too high to ensure a low empyreumatic oil yield. In this work, considering that ozone is a more powerful oxidant than oxygen, it was used to assist the sample carbonization in this experiment to ensure that the sample could be rapidly carbonized at a lower temperature.

Temperature has an important influence on the half-life of ozone. The half-life of ozone in air at 20, 120, and 250 °C is 3 days, 1.5 h, and 1.5 s, respectively [21]. Considering that carbonization was best performed at as high a temperature as possible [22], a carbonization test was conducted at 250 °C. The carbonization conditions were determined by the complete blackening of a 0.2-g citrus leaf and the absence of smoke at the next heating stage.

Initial carbonization experiments were performed with ozone at a flow rate of 100 mL min⁻¹. The effect of temperature experiments were investigated at 150, 200, 250, 300, 350, and 400 °C, respectively. The times for complete carbonization were 15, 10, 8, 8, 7, and 7 min, respectively. When the carbonization temperature was greater than 250 °C, the time for complete carbonization changed very little. Moreover, when the carbonization temperature exceeded 350 °C, a large amount of empyreumatic oil was generated in the sample tube. The effect of the ozone flow rate was investigated at 250 °C with flow rates of 0, 25, 50, 100, 300, 600, and 1000 mL min⁻¹. The carbonization was complete within 30, 15, 10, 8, 8, 6, and 5 min, respectively. As the ozone flow rate increased, the

time for complete carbonization gradually reduced. When the ozone flow rate was greater than 50 mL min^{-1} , the time for complete carbonization changed very little. In addition, when the ozone flow rate was less than 600 mL min^{-1} , the amount of empyreumatic oil produced was very small. When the ozone flow rate was greater than 600 mL min^{-1} , a large amount of empyreumatic oil was located below the sand core. It is possible that when the ozone flow rate was greater than 600 mL min^{-1} , the ozone was able to penetrate the sample zone. The resulting empyreumatic oil moved along with the ozone and condensed at the tube wall below the sand core. When the ozone flow rate was less than 600 mL min^{-1} , the ozone and the empyreumatic oil were blocked by the sample zone above the sand core. Thus, the ozone and the empyreumatic oil were mixed well, and the empyreumatic oil was sufficiently oxidized by ozone. According to these results, considering energy consumption, ozone consumption, and empyreumatic oil production, the optimal carbonization temperature, carbonization time, and ozone flow rate were determined as $250 \text{ }^\circ\text{C}$, 10 min, and 50 mL min^{-1} , respectively.

Oxidation conditions at high temperature

Considering that ozone rapidly decomposes at a higher heating temperature, oxygen was used instead of ozone as an auxiliary oxidizing gas at the oxidation stage. From the carbonization experiments, with an ozone flow rate of 600 mL min^{-1} , the empyreumatic oil was present below the sand core. This indicates that the gas could completely penetrate the sample zone. Thus, the flow rate of oxygen in the oxidation stage was also selected as 600 mL min^{-1} .

Initial experiments were performed to select the oxidation temperature and time by detection of residual organic matter (ROM). According to our reported method [13], the determination of acid-insoluble residue (AIR) could indirectly show changes in organic matter residues. Therefore, preliminary experiments were performed to select the ashing temperature and time by detection of AIR after ashing of a citrus leaf by the AFIA. Citrus leaf was ashed at 500, 600, 700, and $800 \text{ }^\circ\text{C}$ for 5, 10, 20, 30, and 40 min, respectively. To reduce the error, 12 samples of 0.2 g citrus leaf were simultaneously ashed under the same conditions. All the ashes were dissolved in 10% (v/v) nitric acid and cleaned with deionized water. The residues were dried and weighed. The level of the residual organic matter was evaluated by calculation of the ratio of AIR to the total mass of the sample. The ratio of AIR decreased rapidly as the oxidation temperature and the oxidation time increased. When the oxidation temperature was more than $600 \text{ }^\circ\text{C}$ and the oxidation time exceeded 20 min, the ratio of AIR remained essentially unchanged. Therefore, taking into account the energy efficiency ratio, an oxidation temperature of $600 \text{ }^\circ\text{C}$ and an oxidation time of 20 min were selected as the preliminary conditions.

Removal of the empyreumatic oil

To eliminate the interference of the organic matter with ICP-MS measurement and facilitate the cleaning of the ashing tube, it is necessary to remove the empyreumatic oil from the ashing tube by pyrolysis. Because a small amount of the empyreumatic oil produced during the previous two heating stages accumulated below the sample holder, the ashing tube was moved up to 30 mm so that the empyreumatic oil was in the center of the heating zone. In addition, according to our previous report [13], the empyreumatic oil could be easily removed by pyrolysis at $600 \text{ }^\circ\text{C}$. The pyrolysis time and the oxygen flow rate were also optimized. The pyrolysis experiments were performed with oxygen flow rates of 50, 100, 200, 400, and 600 mL min^{-1} . When the oxygen flow rate was more than 100 mL min^{-1} , the empyreumatic oil could be easily removed by pyrolysis within 5 min. Taking cost saving into consideration, 100 mL min^{-1} was selected as the optimal oxygen flow rate to remove the empyreumatic oil.

Dissolution of the ash and homogenization of the solution

Twenty-five milliliters of 10% (v/v) nitric acid was automatically and quantitatively added into the inner tube through syringe pumps to dissolve the ash. An ultrasonic wave was used as an auxiliary means to accelerate the dissolution of ash and the homogenate of the solution, based on the cavitation effect of ultrasound [23]. To make the solution of the inner tube and the solution of the outer tube mix uniformly, the dilute nitric acid in the inner tube was pressed into the outer tube by the blowing of oxygen into the inner tube through a gas module. If the gas flow rate is too low, the liquid level in the inner tube will drop very slowly. In contrast, if the gas flow rate is too high, the liquid level in the outer tube will be raised rapidly, which may cause the solution to overflow from the upper end of the ashing tube. Therefore, the gas flow rate in the inner tube was also optimized. When the gas flow rate was more than 300 mL min^{-1} , the solution was able to overflow from the upper end of the ashing tube. Therefore, taking into account the efficiency of dissolution, 250 mL min^{-1} was chosen as the oxygen flow rate. At a flow rate of 250 mL min^{-1} , the oxygen could smoothly move down from the inner tube and then it gently and evenly overflowed from the inner tube to the outer tube in the form of bubbles. The movement of the bubbles acts as a mechanical agitation of the solution and homogenizes the solution. After the ashing tube had been placed in an ultrasonic bath and oxygen had been blown in for 3 min, the ash was completely dissolved.

Table 2 Comparison between the proposed method and microwave digestion

Method	Theory	Advantages and disadvantages	Samples per batch	Time per batch	Accuracy and precision	Applicable sample types
Proposed method	Dry ashing	Advantages: automation; requires only a small amount of dilute acid; environment friendly Disadvantages: the loss of volatile elements; not suitable for liquid samples and Si-enriched samples	12	40 min (including carbonization, ashing, dissolution, homogenization, constant volume)	The recoveries of some elements easy wrapped by Si may be low for Si-enriched samples The loss of volatile elements such as As, Se, and Hg at high temperature Automated operation reduces errors from manual operation	High organic matter samples; animal, plant, biological tissue
Microwave digestion	Wet digestion	Advantages: Sealed system; low contamination risk Disadvantages: manual operation; high cost of instrument; explosion risk for digestion vessels; samples with high organic matter need overnight predigestion; need to drive off acid; environmental pollution	About 15	>1 h (including microwave heating, decompression, driving off acid and constant volume; not including overnight predigestion)	The sample may be contaminated in the process of driving off acid Manual operation may lead to errors	Animal/human tissue, plant, soil, ore, inorganic materials

Comparison between AFIA and microwave digestion for pretreatment of biological samples

Microwave digestion is a powerful method for the pretreatment of biological samples. The digestion processes in microwave digestion are sealed. The sample needs to be predigested overnight before being digested in a microwave oven. Because the acidity of the digestion solution is very high, the digestion solution needs to be heated to drive off the

excess acid before being measured by the apparatus. Therefore, microwave digestion also causes some acid pollution of the environment. Moreover, the whole pretreatment process takes a very long time, and the instrument for microwave digestion is very expensive. The proposed method uses focused infrared radiation to heat only the part of the ashing tube that contains samples, and thus has a high heating rate and a high ashing efficiency. Only a small amount of dilute acid is needed. The whole process from solid sample to liquid

Table 3 The method detection limits (MDLs)

Element and line or mass	MDL (ng g ⁻¹)	Element and line or mass	MDL (ng g ⁻¹)	Element and line or mass	MDL (ng g ⁻¹)
Ca (317.9 nm)	14.6 ^a	Zn (66 amu)	87	Eu (153 amu)	0.56
Mg (285.2 nm)	1.75 ^a	Rb (85 amu)	2.65	Gd (157 amu)	2.16
Na (588.9 nm)	5.25 ^a	Sr (88 amu)	30	Tb (159 amu)	0.61
P (213.6 nm)	7.91 ^a	Y (89 amu)	1.81	Dy (163 amu)	1.41
Li (7 amu)	5.6	Mo (95 amu)	4.1	Ho (165 amu)	0.55
Be (9 amu)	1.04	Ag (107 amu)	0.50	Er (166 amu)	0.48
Sc (45 amu)	5.76	Cs (133 amu)	1.64	Tm (169 amu)	0.32
Ti (47 amu)	110	Ba (137 amu)	70	Yb (172 amu)	0.77
V (51 amu)	35	La (139 amu)	2.48	Lu (175 amu)	0.22
Mn (55 amu)	51	Ce (140 amu)	2.48	Tl (205 amu)	15.3
Co (59 amu)	4.59	Pr (141 amu)	0.57	Th (232 amu)	1.23
Ni (60 amu)	22	Nd (146 amu)	2.91	U (238 amu)	1.34
Cu (63 amu)	45	Sm (147 amu)	1.64		

The sample mass is 0.2 g, and the final solution volume is 25 mL.

^a The unit is micrograms per gram.

Table 4 The analytical results of eight certified reference materials of biological samples obtained by use of the automated focused infrared microashing sample preparation system combined with inductively coupled plasma optical emission spectroscopy and inductively coupled plasma mass spectrometry

Element/ unit	Type of value	Citrus leaf (GBW10020)	Bush leaf (GBW07603)	Scallion (GBW10049)	Astragalus (GBW10028)	Laver (GBW10023)	Maize (GBW10012)	Human hair (GBW09101b)	Scallop (GBW10024)
Ca/10 ⁻²	Certified	4.2±0.4	1.68±0.11	2.28±0.09	0.456±0.018	0.153±0.018	0.0055±0.0008	0.154±0.007	0.075±0.009
	Obtained	4.15±0.20	1.61±0.03	2.13±0.09	0.44±0.03	0.18±0.02	0.0068±0.0008	0.17±0.01	0.088±0.008
	RE (%)	1.2	4.3	6.0	2.6	17.3	24.4	12.9	17.2
Mg/10 ⁻²	Certified	0.234±0.007	0.48±0.04	0.27±0.01	0.228±0.010	0.40±0.01	0.018±0.002	0.0248±0.0014	0.174±0.006
	Obtained	0.21±0.01	0.42±0.02	0.23±0.01	0.20±0.01	0.34±0.01	0.020±0.001	0.027±0.002	0.16±0.01
	RE (%)	11.5	13.0	15.5	11.6	15.3	9.8	9.2	9.3
Na/μg g ⁻¹	Certified	130±20	19,600±1800	300	1450±190	15,500±600	(10)	445±40	4600±400
	Obtained	142±8	17,067±359	338±14	1263±61	13,533±364	85±16	402±28	3895±43
	RE (%)	9.2	12.9	12.6	12.9	12.7	–	9.7	15.3
P/10 ⁻²	Certified	0.125±0.009	0.1±0.004	0.36±0.02	0.225±0.012	0.585±0.040	0.061±0.003	0.0174±0.0043	0.88±0.07
	Obtained	0.12±0.01	0.093±0.002	0.33±0.01	0.20±0.01	0.50±0.02	0.054±0.001	0.014±0.001	0.78±0.01
	RE (%)	7.1	7.2	9.4	12.0	14.5	11.4	19.1	11.8
Li/μg g ⁻¹	Certified	1.0±0.1	2.6±0.4	1.6±0.2	1.25±0.12	2.36±0.15	0.038±0.006	–	0.13±0.02
	Obtained	0.94±0.04	2.81±0.08	1.89±0.02	1.35±0.12	2.49±0.15	0.032±0.005	0.78±0.14	0.12±0.02
	RE (%)	5.6	8.0	18.0	8.4	5.6	16.1	–	7.2
Be/μg g ⁻¹	Certified	31±7	51±4	59±11	50±14	115±14	1.7±0.4	–	3.2±0.7
	Obtained	26±1	45±2	48±2	43±3	94±3	2.08±0.10	ND	3.33±0.45
	RE (%)	17.7	11.1	19.1	14.1	18.3	22.6	–	4.2
Sc/μg g ⁻¹	Certified	0.140±0.020	0.32±0.04	(0.26)	(0.3)	(0.49)	0.0035±0.0009	–	(0.012)
	Obtained	0.15±0.01	0.51±0.05	0.36±0.01	0.32±0.04	0.57±0.03	ND	0.015±0.002	0.013±0.001
	RE (%)	7.7	58.4	–	–	–	–	–	–
Ti/μg g ⁻¹	Certified	38±10	95±20	(62)	102±11	(92)	1.6±0.5	(2.1)	(6)
	Obtained	30±1	78±6	53±5	72±4	55±4	1.77±0.27	2.24±0.12	6.26±0.23
	RE (%)	22.3	17.8	–	29.7	–	10.8	–	–
V/μg g ⁻¹	Certified	1.16±0.13	2.4±0.4	(3)	2.56±0.32	4.2±0.6	0.30±0.11	(0.089)	0.36±0.10
	Obtained	0.89±0.07	2.16±0.19	3.64±0.39	2.37±0.23	4.42±0.51	0.37±0.06	0.13±0.02	0.46±0.07
	RE (%)	23.5	9.8	–	7.6	5.3	23.0	–	26.7
Mn/μg g ⁻¹	Certified	30.5±1.5	61±5	173±7	33±1	68±3	1.55±0.08	3.83±0.39	19.2±1.2
	Obtained	29±1	58±2	166±10	30±1	60±2	1.71±0.16	3.24±0.25	20.0±0.4
	RE (%)	4.3	5.7	3.9	9.7	12.5	10.4	15.4	6.4
Co/μg g ⁻¹	Certified	0.23±0.06	0.41±0.05	0.59±0.04	0.44±0.03	0.63±0.05	(0.012)	0.153±0.015	0.047±0.006
	Obtained	0.16±0.01	0.35±0.02	0.43±0.03	0.36±0.05	0.46±0.02	0.014±0.003	0.12±0.01	0.044±0.003
	RE (%)	29.5	15.2	27.8	18.4	26.3	–	22.5	5.9
Ni/μg g ⁻¹	Certified	1.1	1.7±0.3	(1.9)	2.26±0.15	2.25±0.18	0.097±0.014	(5.77)	0.29±0.08
	Obtained	1.12±0.08	1.44±0.15	1.53±0.08	1.85±0.25	2.20±0.02	0.085±0.012	4.04±0.19	0.25±0.03
	RE (%)	2.1	15.5	–	18.2	2.3	11.9	–	14.4
Cu/μg g ⁻¹	Certified	6.6±0.5	6.6±0.8	5.5±0.3	8.5±0.7	12.2±1.1	0.66±0.08	33.6±2.3	1.34±0.18
	Obtained	5.51±0.07	5.94±0.5	5.13±0.26	7.34±0.73	9.94±1.23	0.60±0.10	28±2	1.21±0.18
	RE (%)	16.5	10.0	6.8	13.6	18.5	9.0	17.3	10.1
Zn/μg g ⁻¹	Certified	18±2	55±4	25±1	22.3±1.0	28±2	2.9±0.3	191±16	75±3
	Obtained	18.7±0.3	56±5	24±1	26±1	33±2	3.57±0.59	179±8	87±2
	RE (%)	4.1	2.6	2.5	18.2	17.5	23.1	6.1	15.9
Rb/μg g ⁻¹	Certified	3.0±0.2	4.5±0.6	9.4±0.8	10.5±0.5	10.4±0.7	2.1±0.2	(0.06)	5.1±0.3
	Obtained	2.28±0.08	4.03±0.04	7.68±0.19	8.83±1.28	10.1±0.8	1.75±0.11	0.14±0.01	4.81±0.18
	RE (%)	24.0	10.5	18.4	15.9	2.8	16.6	–	5.7
Sr/μg g ⁻¹	Certified	170±10	246±16	74±5	51±3	24±2	0.19±0.05	8.17±0.69	6.5±0.4

Table 4 (continued)

Element/ unit	Type of value	Citrus leaf (GBW10020)	Bush leaf (GBW07603)	Scallion (GBW10049)	Astragalus (GBW10028)	Laver (GBW10023)	Maize (GBW10012)	Human hair (GBW09101b)	Scallop (GBW10024)
Y/ $\mu\text{g g}^{-1}$	Obtained	165±9	232±16	70±3	50±5	23±2	0.24±0.04	8.98±0.49	6.45±0.02
	RE (%)	2.7	5.6	5.8	1.7	3.5	27.2	10.0	0.8
	Certified	0.42±0.04	(0.63)	0.61±0.14	0.6±0.1	6.6±1.3	0.021±0.004	–	0.107±0.012
Mo/ $\mu\text{g g}^{-1}$	Obtained	0.30±0.02	0.54±0.03	0.46±0.03	0.50±0.04	5.31±0.52	0.024±0.004	0.014±0.002	0.098±0.004
	RE (%)	29.1	–	25.2	16.9	19.5	13.1	–	8.9
	Certified	0.20±0.01	0.28±0.05	0.12±0.03	5.7±0.6	0.78±0.09	0.045±0.009	1.06±0.12	0.066±0.016
Ag/ ng g^{-1}	Obtained	0.19±0.01	0.31±0.01	0.12±0.01	5.86±0.17	0.78±0.03	0.054±0.006	0.93±0.02	0.068±0.006
	RE (%)	3.6	10.4	3.2	2.8	0.7	19.1	12.3	3.0
	Certified	54±5	49	14	(8)	73	–	37±2	(8)
Cs/ $\mu\text{g g}^{-1}$	Obtained	40±4	49±4	14.2±2.4	8.50±0.90	69±1	5.31±3.20	26±2	7.52±0.51
	RE (%)	26.5	0.1	1.2	–	5.5	–	29.2	–
	Certified	0.14±0.01	0.27±0.02	0.19±0.02	0.235±0.014	0.35±0.03	0.010±0.004	–	0.014±0.001
Ba/ $\mu\text{g g}^{-1}$	Obtained	0.11±0.01	0.25±0.02	0.16±0.01	0.22±0.02	0.26±0.02	0.011±0.001	0.010±0.005	0.016±0.001
	RE (%)	21.4	9.1	16.0	5.1	25.5	12.5	–	14.6
	Certified	98±6	18±2	36±5	20.5±2.5	10.4±1.5	0.45±0.16	–	0.62±0.06
La/ $\mu\text{g g}^{-1}$	Obtained	120±4	15.2±0.4	32±1	15.6±1.1	10.6±0.8	0.56±0.05	11.3±1.3	0.77±0.07
	RE (%)	22.4	15.6	11.9	24.0	1.5	24.4	–	24.5
	Certified	0.57±0.06	1.25±0.06	1.16±0.10	1.07±0.09	3.4±0.3	0.057±0.006	(0.029)	0.037±0.008
Ce/ $\mu\text{g g}^{-1}$	Obtained	0.448±0.029	1.017±0.038	0.931±0.061	0.838±0.056	2.878±0.179	0.06±0.006	0.031±0.002	0.036±0.003
	RE (%)	21.32	18.66	19.77	21.68	15.35	4.85	–	3.38
	Certified	1.00±0.13	2.2±0.1	2.1±0.3	2.03±0.23	4.7±0.2	0.12±0.02	–	0.053±0.013
Pr/ ng g^{-1}	Obtained	0.75±0.06	1.93±0.05	1.60±0.06	1.58±0.07	4.09±0.25	0.13±0.01	0.066±0.025	0.054±0.002
	RE (%)	25.3	12.3	23.8	22.4	12.9	9.1	–	2.5
	Certified	108±14	240	235±29	231±28	800±42	7±1	–	6.0±0.8
Nd/ $\mu\text{g g}^{-1}$	Obtained	97±9	180±12	188±20	194±19	600±53	8.40±0.79	6.61±0.54	5.50±0.58
	RE (%)	10.0	24.9	20.2	16.2	25.1	19.9	–	8.3
	Certified	0.42±0.05	1±0.1	0.91±0.11	0.90±0.11	3.1±0.2	0.022±0.004	–	0.025±0.007
Sm/ ng g^{-1}	Obtained	0.38±0.02	0.86±0.06	0.70±0.05	0.66±0.04	3.03±0.16	0.028±0.002	0.036±0.014	0.025±0.002
	RE (%)	9.7	14.3	23.5	26.4	2.1	26.0	–	1.5
	Certified	80±7	190±20	167±18	172±13	(81)	3.2±0.5	–	4.8±1.5
Eu/ ng g^{-1}	Obtained	69±4	168±10	128±10	126±10	662±41	4.13±0.43	4.13±0.54	4.24±0.44
	RE (%)	13.7	11.4	23.5	27.0	–	28.9	–	11.7
	Certified	(33)	39±3	39±4	32±6	126±10	(0.6)	–	0.9±0.3
Gd/ ng g^{-1}	Obtained	25±3	31±3	28±2	25±2	121±5	1.25±0.21	1.90±0.53	1.05±0.16
	RE (%)	–	20.1	27.4	21.6	3.7	–	–	16.7
	Certified	81±10	190	155±34	160±18	760±75	4.3±0.9	–	5.2±1.2
Tb/ ng g^{-1}	Obtained	66±6	158±12	118±14	115±10	745±44	5.20±1.11	3.40±0.75	4.58±0.71
	RE (%)	18.9	16.6	23.7	28.4	2.0	20.9	–	11.9
	Certified	11±1	25±3	22±5	22±2	110±10	0.73±0.24	–	0.84±0.19
Dy/ ng g^{-1}	Obtained	8.73±0.28	26±1	17.7±0.7	17.3±1.3	107±9	ND	ND	0.73±0.15
	RE (%)	20.6	2.9	19.8	21.3	2.5	–	–	13.1
	Certified	57±5	(130)	119±12	122±13	654±66	3.2±0.8	20±7	5.3±1.2
Ho/ ng g^{-1}	Obtained	48±5	116±10	97±14	95±8	634±36	3.52±1.24	2.86±0.41	5.12±0.89
	RE (%)	16.0	–	18.5	22.0	3.1	10.0	–	3.4
	Certified	11±1	33	22±4	23±4	126±22	0.66±0.15	–	1.2±0.3
Er/ ng g^{-1}	Obtained	8.76±0.46	30±2	22±2	17.2±0.8	117±10	0.81±0.11	ND	1.31±0.23
	RE (%)	20.3	9.7	2.1	25.3	7.3	22.5	–	9.4
	Certified	26±6	–	57±12	60±12	312±30	1.7±0.4	–	3.3±0.7

Table 4 (continued)

Element/ unit	Type of value	Citrus leaf (GBW10020)	Bush leaf (GBW07603)	Scallion (GBW10049)	Astragalus (GBW10028)	Laver (GBW10023)	Maize (GBW10012)	Human hair (GBW09101b)	Scallop (GBW10024)
Tm/ng g ⁻¹	Obtained	25±1	72±7	52±4	47±4	288±14	2.10±0.21	1.85±0.27	3.47±0.24
	RE (%)	5.2	–	8.9	21.8	7.7	23.3	–	5.2
	Certified	3.8±0.9	–	7.8±1.5	8.8±1.8	43±8	(0.27)	–	0.52±0.10
Yb/ng g ⁻¹	Obtained	3.75±0.35	8.75±0.51	7.5±0.87	7.81±1.16	35±2	ND	ND	0.45±0.07
	RE (%)	1.3	–	3.9	11.3	17.6	–	–	14.1
	Certified	25±5	63±14	57±17	62±19	253±35	1.6±0.2	–	3.2±0.9
Lu/ng g ⁻¹	Obtained	21±3	58±4	42±3	45±1	227±6	2.01±0.23	1.67±0.36	3.02±0.21
	RE (%)	17.8	8.1	26.6	27.2	10.2	25.6	–	5.6
	Certified	3.7±0.9	11	(8)	9±3	38±3	(0.21)	–	0.49±0.11
Tl/ng g ⁻¹	Obtained	2.51±0.26	7.92±0.68	7.92±1.18	6.67±0.59	35±2	ND	ND	0.42±0.06
	RE (%)	32.4	28.0	–	25.9	6.8	–	–	15.0
	Certified	60±8	–	37±8	51±6	44±4	(0.4)	–	2.5±0.4
Th/ng g ⁻¹	Obtained	48±4	19.9±2.4	29±2	40±3	43±6	ND	ND	ND
	RE (%)	19.4	–	22.6	20.9	3.4	–	–	–
	Certified	140±20	360±40	364±58	300±40	730±50	4.6±1.5	–	12
U/ng g ⁻¹	Obtained	125±14	324±26	352±31	315±29	716±151	5.40±0.63	10.6±3.5	13.2±1.6
	RE (%)	11.7	11.2	3.4	4.7	1.9	14.8	–	9.1
	Certified	45±10	120	(50)	122±14	172±18	(2.3)	–	7.3±1.3
	Obtained	39±10	118±25	44±7	113±9	158±13	2.64±0.35	9.47±1.17	8.44±1.12
	RE (%)	14.9	2.1	–	8.3	9.2	–	–	13.5

The results are expressed as the mean ± standard deviation ($n = 5$, five parallel samples for each material). The values in parentheses are reference values. *ND* not detected, *RE* relative error.

solution is completed by unattended operation. Table 2 in a clearer manner shows a comparison between microwave digestion and the proposed method.

Analytical applications

As an automated instrument for sample preparation, the performance of the AFIA was evaluated by method detection limits (MDLs), method precision, and method accuracy based on the established analytical method combined with ICP-OES and ICP-MS.

The MDLs were calculated as the concentration corresponding to three times the standard deviation of 20 independent sample blanks divided by the slope of the analytical curve (confidence level 99.6%) [24], and the results are listed in Table 3. The method precision and the method accuracy were evaluated by our analyzing eight biological certified reference materials (GBW10020 citrus leaf, GBW07603 bush leaf, GBW10049 scallion, GBW10028 astragalus, GBW10023 laver, GBW10012 maize, GBW09101b human hair, and GBW10024 scallop), which were ashed with the AFIA under the optimized conditions and analyzed by ICP-OES and ICP-MS. The results obtained for the 38 elements Ca, Mg, Na, P, Li, Be, Sc, Ti, V, Mn, Co, Ni, Cu, Zn, Rb, Sr, Y, Mo, Ag, Cs, Ba, Tl, Th, U, and rare earth elements, are shown in Table 4.

The relative errors for the 38 elements between the certified and the obtained values were typically less than 30%, and the relative standard deviations of five replicates were typically below 15%, which complied with the Chinese specification of the regional ecogeochemistry assessment standard [25].

Conclusions

A focused infrared ashing system was proposed. It has the property of fully automated operation of the whole ashing process, including charring, ashing, dissolution, and homogenization. The whole process was run unattended within 40 min, while avoiding the errors caused by manual operation. Ozone accelerated the carbonization at low temperature to increase the carbonization efficiency. The use of a double-layer tube as the only container in the whole process reduced the risk of pollution.

Funding This study was funded by the National Instrumentation Program of China (grant no. 2013YQ510391), the Shaanxi Province Science and Technology Project (grant no. 2015GY054), the National Science Fund of China (grant no. 21575113), the Specialized Research Fund for the Doctoral Program of Higher Education (grant no. 20126101110013), and the Scientific Research Foundation of Shaanxi Provincial Key Laboratory (grant nos 15JS100 and 16JS099).

Compliance with ethical standards

Conflict of interest The authors declare that they have no competing interests.

Ethics statement This article does not contain any studies with human participants or animals performed by any of the authors. The human hair sample used in this work was a Chinese national certified reference standard material, which was purchased from a commercial institute in China.

References

1. Steehler JK. Sample preparation techniques in analytical chemistry (Mittra, Somenath). *J Chem Educ.* 2004;81:199. <https://doi.org/10.1021/ed081p199>.
2. Bizzi CA, Pedrotti MF, Silva JS, Barin JS, Nóbrega JA. Microwave-assisted digestion methods: towards greener approaches using plasma-based techniques. *J Anal At Spectrom.* 2017;32:1448–66. <https://doi.org/10.1039/C7JA00108H>.
3. Pereira LSF, Frohlich AC, Duarte FA, Burrow RA, Muller EI. Determination of halogens and sulfur in pitch from crude oil by plasma-based techniques after microwave-induced combustion. *J Anal At Spectrom.* 2015;30:1822–7. <https://doi.org/10.1039/C5JA00143A>.
4. Barin JS, Mello PA, Mesko MF, Duarte FA, Flores EM. Determination of elemental impurities in pharmaceutical products and related matrices by ICP-based methods: a review. *Anal Bioanal Chem.* 2016;408:4547–66. <https://doi.org/10.1007/s00216-016-9471-6>.
5. Costa VC, Picoloto RS, Hartwig CA, Mello PA, Flores EM. Feasibility of ultra-trace determination of bromine and iodine in honey by ICP-MS using high sample mass in microwave-induced combustion. *Anal Bioanal Chem.* 2015;407:7957–64. <https://doi.org/10.1007/s00216-015-8967-9>.
6. Matusiewicz H. Sample decomposition techniques in inorganic trace elemental analysis. In: Baranowska B, editor. *Handbook of trace analysis: fundamentals and applications.* Cham: Springer; 2016. p. 75–122.
7. Shen K, Zhang N, Yang X, Li Z, Zhang Y, Zhou T. Dry ashing preparation of (quasi)solid samples for the determination of inorganic elements by atomic/mass spectrometry. *Appl Spectrosc Rev.* 2015;50:304–31. <https://doi.org/10.1080/05704928.2014.986735>.
8. Yamada N. Kinetic energy discrimination in collision/reaction cell ICP-MS: theoretical review of principles and limitations. *Spectrochim Acta Part B At Spectrosc.* 2015;110:31–44. <https://doi.org/10.1016/j.sab.2015.05.008>.
9. Grindlay G, Mora J, de Loos-Vollebregt M, Vanhaecke F. A systematic study on the influence of carbon on the behavior of hard-to-ionize elements in inductively coupled plasma–mass spectrometry. *Spectrochim Acta Part B At Spectrosc.* 2013;86:42–9. <https://doi.org/10.1016/j.sab.2013.05.002>.
10. Avila Orozco FD, Kovachev N, Aguirre Pastor MÁ, Domini CE, Fernández Band BS, Canals Hernández A. Analysis of metals and phosphorus in biodiesel B100 from different feedstock using a Flow Blurring® multinebulizer in inductively coupled plasma-optical emission spectrometry. *Anal Chim Acta.* 2014;827:15–21. <https://doi.org/10.1016/j.aca.2014.04.016>.
11. Enders A, Lehmann J. Comparison of wet-digestion and dry-ashing methods for total elemental analysis of biochar. *Commun Soil Sci Plant Anal.* 2012;43:1042–52. <https://doi.org/10.1080/00103624.2012.656167>.
12. Azcue J, Mudroch A. Comparison of different washing, ashing, and digestion methods for the analysis of trace elements in vegetation. *Int J Environ Anal Chem.* 1994;57:151–62. <https://doi.org/10.1080/03067319408027420>.
13. Zhang N, Li Z, Zheng J, Yang X, Shen K, Zhou T, et al. Multielemental analysis of botanical samples by ICP-OES and ICP-MS with focused infrared lightwave ashing for sample preparation. *Microchem J.* 2017;134:68–77. <https://doi.org/10.1016/j.microc.2017.05.006>.
14. Revelli JF, Disalvo FJ. Tantalum disulfide (TaS₂) and its intercalation compounds. In: Murphy DW, Interrante LV, editors. *Inorganic syntheses: nonmolecular solids, vol 30.* Hoboken: Wiley; 1979. p. 155–69. <https://doi.org/10.1002/9780470132616.ch32>.
15. Capelo-Martínez JL, Ximénez-Embun P, Madrid Y, Camara C, Capelo-Martínez JL, Ximénez-Embun P, et al. Advanced oxidation processes for sample treatment in atomic spectrometry. *Trends Anal Chem.* 2004;23:331–40. [https://doi.org/10.1016/s0165-9936\(04\)00401-7](https://doi.org/10.1016/s0165-9936(04)00401-7).
16. General Administration of Quality Supervision, Inspection and Quarantine of the People's Republic of China. Laboratory sintered (fritted) filters-Porosity grading, classification and designation. National Standard of China, Standard No.GB/T 11415. 1989. <http://www.gb688.cn/bzgk/gb/newGbInfo?hcno=5966CEFF486436ABA16B94F6BAABF8FC>.
17. Novotnik B, Zuliani T, Martinčić A, Ščanar J, Milačić R. Effective reduction of polyatomic interferences produced by high chloride and carbon concentrations in determination of Cr(VI) by FPLC-ICP-MS. *J Anal At Spectrom.* 2012;27:488. <https://doi.org/10.1039/c2ja10270f>.
18. Gleit CE, Holland WD. Use of electrically excited oxygen for the low temperature decomposition of organic substances. *Anal Chem.* 1962;34:1454–7. <https://doi.org/10.1021/ac60191a031>.
19. Hill AD, Patterson KY, Veillon C, Morris ER. Digestion of biological materials for mineral analyses using a combination of wet and dry ashing. *Anal Chem.* 1986;58:2340–2. <https://doi.org/10.1021/ac00124a049>.
20. IUPAC. *Compendium of chemical terminology*, 2nd ed. (the "Gold Book"). Compiled by A. D. McNaught and A. Wilkinson. Oxford: Blackwell Scientific Publications; 1997. XML on-line corrected version: <http://goldbook.iupac.org> (2006-) created by M. Nic, J. Jirat, B. Kosata; updates compiled by A. Jenkins. <https://doi.org/10.1351/goldbook>
21. Bataklijev T, Georgiev V, Anachkov M, Rakovsky S, Rakovsky S. Ozone decomposition. *Interdiscip Toxicol.* 2014; <https://doi.org/10.2478/intox-2014-0008>.
22. Dhandapani B, Oyama ST. Gas phase ozone decomposition catalysts. *Appl Catal B Environ.* 1997;11:129–66. [https://doi.org/10.1016/S0926-3373\(96\)00044-6](https://doi.org/10.1016/S0926-3373(96)00044-6).
23. Peshkovsky AS, Peshkovsky SL. *Acoustic cavitation theory and equipment design principles for industrial applications of high-intensity ultrasound.* Nova, Hauppauge. 2010.
24. Freiser H, Nancollas GH. *Compendium of analytical nomenclature (definitive rules 1987)*. 2nd ed. Oxford: Blackwell; 1987. p. 8–11.
25. Ministry of Land and Resources of the People's Republic of China. *Specification of regional ecogeochemistry assessment. Geology and mineral industry standard of China.* Standard No. DZ/T 0289. 2015. http://www.mlr.gov.cn/zwgk/zytz/201510/t20151013_1383877.htm.